

Bayesian experimental design of a multichannel interferometer for Wendelstein 7-Xa)

H. Dreier, A. Dinklage, R. Fischer, M. Hirsch, and P. Kornejew

Citation: [Review of Scientific Instruments](#) **79**, 10E712 (2008); doi: 10.1063/1.2956962

View online: <http://dx.doi.org/10.1063/1.2956962>

View Table of Contents: <http://scitation.aip.org/content/aip/journal/rsi/79/10?ver=pdfcov>

Published by the [AIP Publishing](#)

Articles you may be interested in

[Diagnostics design for steady-state operation of the Wendelstein 7-X stellarator](#))

Rev. Sci. Instrum. **81**, 10E133 (2010); 10.1063/1.3483210

[Optical design study of an infrared visible viewing system for Wendelstein 7-X divertor observation and control](#))

Rev. Sci. Instrum. **79**, 10F513 (2008); 10.1063/1.2979880

[Design and Calibration of a Polychromator for the Thomson Scattering at Wendelstein 7-X](#)


AIP Conf. Proc. **993**, 195 (2008); 10.1063/1.2909107

[Design and Study of the Observation Optics for the Thomson Scattering Planned at Wendelstein 7-X](#)


AIP Conf. Proc. **993**, 191 (2008); 10.1063/1.2909106

[Integrating diagnostic data analysis for W 7- AS using Bayesian graphical models](#)

Rev. Sci. Instrum. **75**, 4219 (2004); 10.1063/1.1789611

The logo for JANIS, consisting of the letters 'JANIS' in a large, blue, serif font.

Does your research require low temperatures? Contact Janis today.
Our engineers will assist you in choosing the best system for your application.

Five images of different cryogenic systems: 1. A vertical cryocooler with a silver finish. 2. A cryostat with a yellow top and silver base. 3. A dilution refrigerator with a silver top and white base. 4. A micro-manipulated probe station with a silver top and white base. 5. A magnet system with a black frame and silver components.

10 mK to 800 K
Cryocoolers
Dilution Refrigerator Systems
Micro-manipulated Probe Stations

LHe/LN₂ Cryostats
Magnet Systems

sales@janis.com **www.janis.com**
Click to view our product web page.

Bayesian experimental design of a multichannel interferometer for Wendelstein 7-X^{a)}

H. Dreier,¹ A. Dinklage,¹ R. Fischer,² M. Hirsch,¹ and P. Kornejew¹

¹Max-Planck-Institut für Plasmaphysik, EURATOM Association, Teilinstitut Greifswald, D-174891 Greifswald, Germany

²Max-Planck-Institut für Plasmaphysik, EURATOM Association, Boltzmannstr. 2, D-85748 Garching, Germany

(Presented 13 May 2008; received 12 May 2008; accepted 23 May 2008; published online 31 October 2008)

Bayesian experimental design (BED) is a framework for the optimization of diagnostics basing on probability theory. In this work it is applied to the design of a multichannel interferometer at the Wendelstein 7-X stellarator experiment. BED offers the possibility to compare diverse designs quantitatively, which will be shown for beam-line designs resulting from different plasma configurations. The applicability of this method is discussed with respect to its computational effort. © 2008 American Institute of Physics. [DOI: 10.1063/1.2956962]

I. DIAGNOSTIC DESIGN USING PROBABILITY THEORY

Future fusion experiments, such as ITER or Wendelstein 7-X, are characterized by a complex interaction of scientific and technical requirements. As a result, a combination of physical questions of interest and technical boundary conditions has to be taken into account for the design of the diagnostic setup.

To ensure the gain of maximum information about the physical parameters of interest, a method for the optimization of plasma diagnostics has to take into account these conditions. A probabilistic approach is given by *Bayesian experimental design* (BED), which offers a consistent mathematical ansatz independent of the diagnostic type and the physical question to be addressed.

The figure of merit is a *utility function* $U(D, \eta)$ (see Ref. 1 for discussion), which depends on the data D of future experiments and the design parameters η . These design parameters describe the diagnostic unit to be optimized, e.g., the geometry of the line-of-sight configuration of an interferometer. Because future data are unknown, the utility function is marginalized over the expected data space, the *expected utility* (EU) reads as

$$EU(\eta) = \int dD U(D, \eta) p(D|\eta). \quad (1)$$

Here, $p(D)$ is a probability density function, describing a weight function for future D from a given diagnostic design η . The marginalization theorem applied here, i.e., the integration over the expected data space, is part of the Bayesian probability theory.

A useful choice for the utility function itself is the *Kullback–Leibler distance*

$$U_{KL}(D, \eta) = \int d\theta p(\theta|D, \eta) \log \left[\frac{p(\theta|D, \eta)}{p(\theta)} \right], \quad (2)$$

which describes the information gain about the parameters of interest, θ . The knowledge about θ before the measurement $p(\theta)$ is compared to the state of knowledge after the measurement, $p(\theta|D, \eta)$, where the data D and a design configuration η are given. The parameters of interest are the physical quantities one wants to estimate, e.g., the parameters describing a spatial electron density distribution.

Using Bayes' theorem, the EU from Eq. (1) reads

$$EU(\eta) = \int dD \int d\theta p(D|\theta, \eta) p(\theta) \log \frac{p(D|\theta, \eta)}{p(D|\eta)} \quad (3)$$

and describes the expected information gain for the parameters of interest θ by future measurements, depending on the design configuration η . The EU in this version is an absolute measure for the information gain; it is expressed in bits if the base-2 logarithm is used. The BED is the maximization of the EU with respect to η . The basic principle of BED is proposed by Lindley;² a more detailed explanation of the EU is given, e.g., in Ref. 3.

II. BEAM-LINE DESIGN FOR DIFFERENT PLASMA CONFIGURATIONS IN W7-X

For the interferometer diagnostic at W7-X an infrared system based on a CO₂ laser ($\lambda = 10.6 \mu\text{m}$) is considered in a plane at a toroidal angle of $\Phi \approx 195^\circ$.⁴ In earlier work case studies about the effect of the error statistics on the beam-line design have been presented,⁵ and the beam-line designs for different physical questions have been compared.⁶ These analyses were made for the standard magnetic configuration at W7-X. In this work, the influence of different plasma configurations and of plasma outside the last closed magnetic surface (LCMS) will be studied.

The physical question of interest to be used here as the design criterion is the occurrence of “hollow” electron den-

^{a)}Contributed paper, published as part of the Proceedings of the 17th Topical Conference on High-Temperature Plasma Diagnostics, Albuquerque, New Mexico, May 2008.

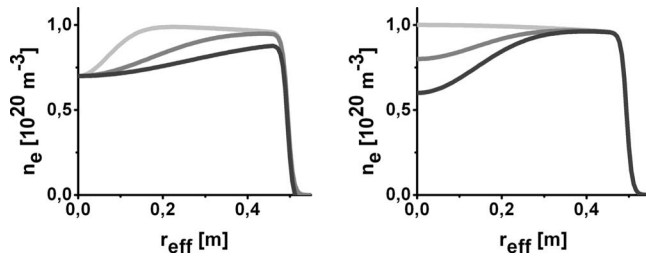


FIG. 1. Assumed variations for two parameters of interest θ : width (left) and depth (right) of the hollow part of the electron density distribution. The maximum density varies from 0.1×10^{20} to $1.0 \times 10^{20} \text{ m}^{-3}$ (not shown).

sity profiles, where the maximum density is not localized in the plasma center. This effect may occur in the case of core electron root confinement (CERC) scenarios. Parameters of interest are the maximum density, the width, and the depth of the hollow part (Fig. 1).

To measure these parameters of interest, a four channel interferometer was optimized, taking into account the technical boundary conditions at W7-X, i.e., the port system and the fixed positions for retroreflectors at the inner wall of the plasma vessel, which are restricted by the structure of the inner wall. Due to the realizable vacuum flange positions at the end of the ports and a limited number of possible positions for retroreflectors, 101 lines of sight were available for probing beam-lines in the interferometry plane of W7-X.

As an additional line of sight, a beam-line congruent to the Thomson scattering diagnostic beam at a toroidal angle of $\Phi \approx 187^\circ$ can be realized. Because this line of sight turns out to be very informative,⁶ it was assumed as given for the following analysis. So only three beams were located at the interferometry plane.

Four different plasma configurations were analyzed for this study: the standard magnetic configuration of W7-X, a high- ι configuration ($\iota=1.2$ at the LCMS), a setup with a significant kinetic pressure of the plasma ($\beta=0.04$), and finally a plasma with a nonvanishing electron density outside the separatrix. For the latter case, an exponential decay of the plasma density was assumed outside the LCMS with a decay length of 5 cm in magnetic coordinates.

Figure 2 shows the results for the optimal beam-line design of the respective plasma configuration with respect to the cross section of the plasma. The beam-line designs for the standard configuration and the high- ι case turn out to be identical; the beam geometry for the other cases varies

TABLE I. EU values (in bits) for different beam-line designs and different plasma configurations: optimal beam-line design for the respective plasma configuration (center column); EU for the CERC beam-line setup (right column).

	Optimal design	CERC design
High- ι plasma	6.741 ± 0.005	6.741 ± 0.005
High- β plasma	6.822 ± 0.005	6.748 ± 0.005
Plasma outside LCMS	6.847 ± 0.005	6.839 ± 0.005

slightly. In all cases, the beam-lines cross the “bulky” part of the plasma cross section, covering the region where the effect of hollowness occurs.

Because only one geometry can be realized in the final diagnostic setup, one has to estimate the beam geometry that is most beneficial for all cases. For this, an important feature of BED can be applied: Because the expected information gain of a design can be estimated, the optimal setup can be found by a quantitative comparison of the different EUs from the various designs.

Table I shows the values of the EU for two cases: the optimal design for the respective plasma configuration as shown in Fig. 2 and the EU for the different plasma configurations when the beam-line design for the standard configuration [Fig. 2(a)] is used. In the case of the high- ι plasma, the EUs are identical (because the beam-line configuration is the same); for the high- β plasma and the case of plasma outside the separatrix, the difference is in the order of 1% of the EU. To conclude, one can state that the beam-line design for the standard magnetic configuration is also a near-to-optimum design for the other plasma configurations analyzed here.

III. COMPUTATIONAL EFFORT

The central element of BED is the calculation of the EU function [Eq. (1)]. For this, the necessary probability density functions need to be estimated first: $p(\theta)$ describes the *area of interest*, i.e., the range of the parameters one is interested in. In the case presented here, the three parameters of interest (maximum density, depth, and width of the hollow part) have been changed uniformly within certain limits. $p(\theta)$ is therefore a three-dimensional uniform distribution. The limits of this distribution are then the limits of the integration over θ .

The likelihood function $p(D|\theta, \eta)$ includes the forward function, a mathematical model function describing the measurement process. It also describes the error statistics of the

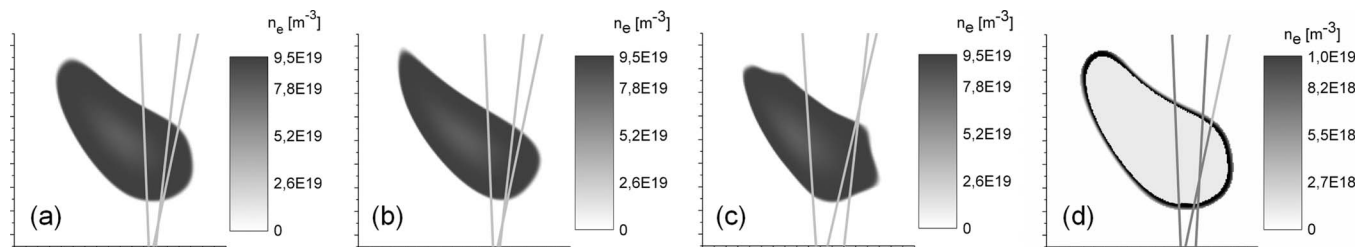


FIG. 2. Plasma cross section in the interferometry plane at W7-X with an optimal beam-line geometry for the measurement of CERC density effects at different plasma configurations: (a) standard configuration for W7-X, (b) high- ι plasma, (c) high- β , and (d) a plasma with an assumed exponential decay of electron density outside the LCMS. For the latter case, the plasma inside the LCMS is shadowed to accentuate the edge plasma.

TABLE II. Computation time for the optimal beam-line configuration of a multichannel interferometer at W7-X with respect to the number of parameters of interest (dimension of θ) and to the number of beam-lines (dimension of D).

No. of parameters of interest	No. of beam-lines	Computation time (min)
3	2	6
3	3	10
3	4	16
4	4	130
5	4	285
5	8	660

future measurement. For the interferometer at W7-X, a constant Gaussian background error was assumed. Because of four interferometry channels, the likelihood turns out to be a four-dimensional Gaussian. The integration over D in Eq. (1) is performed within $[-\infty; \infty]$.

As the final element, the evidence function $p(D|\eta)$ is calculated from the likelihood function and the “interest” function by marginalization,

$$p(D|\eta) = \int d\theta p(\theta) p(D|\theta, \eta). \quad (4)$$

In general, the multidimensional integral in Eq. (1) cannot be solved analytically. The results presented here have been calculated numerically using a simple sampling Monte Carlo algorithm. The computing was done on a multi-CPU blade cluster: two Intel Xeon CPUs (3.06 GHz) with hyper-threading capability located on one blade; 11 blades were used at the same time. The EU was then computed by calculating 100×100 samples in parallel.

For the optimization of the interferometer, only one beam-line was optimized first by calculating its EU for all 101 possible beam positions. Then, the beam-line was fixed at the position with the highest EU value, the next beam-line was estimated the same way, and so on.

Although the parallel computing algorithm was applied, the calculation of the optimal beam-line configuration turned out to be time consuming. As a case study, typical calculation times for one EU value using this method are given in Table II with respect to the number of parameters of interest and the number of beam-lines. The computation time, in particular, depends on the number of parameters of interest be-

cause of the calculation of the evidence function [Eq. (4)]. This function needs to be computed for every Monte Carlo step of the EU calculation, so the dimension of θ has a significant impact on the computation time. The optimization of one four channel interferometer, where three beam-lines were changed (as presented in this work), finally took about 3–5 days in total. It has to be mentioned that these computation times strongly depend on the problem to be solved. In addition to the dimension of θ and D , the forward function, which is an essential part of the likelihood, also plays an important role. In case of the interferometer one has to deal with an integration along the line of sight, resulting in further computational effort. For other diagnostics, e.g., if a linear forward function can be applied, this effort could be reduced significantly.

IV. CONCLUSION

BED as a method for diagnostic design combines several advantages: As a general approach, it is independent of the diagnostic to be optimized. The physical question of interest is implemented directly into the design process by the parameters of interest and their probability density distribution. The quantitative nature of the EU offers the possibility of a direct comparison of different designs, which was used in this work to study the impact of different plasma configurations on the beam-line configuration of a four channel interferometer.

Besides these advantages, it was shown that in the case of nontrivial design problems the computation time may be significant. For a detailed analysis of a physical problem like the one discussed in this work, the overall computation time may take weeks or even months. In such cases, the application of BED will depend on a cost-benefit analysis.

For a fusion experiment like W7-X, which is designed to be a long-run experiment, the optimization of the diagnostics using BED can be recommended to ensure the maximum gain of information from future measurements.

¹K. Chaloner and I. Verdinelli, *Stat. Sci.* **10**, 273 (1995).

²D. V. Lindley, *Bayesian Statistics: A Review* (SIAM, Philadelphia, 1972).

³R. Fischer, *AIP Conf. Proc.* **735**, 76 (2004).

⁴P. Kornejew, M. Hirsch, T. Bindemann, A. Dinklage, H. Dreier, H.-J. Hartfuß, *Rev. Sci. Instrum.* **77**, 10F128 (2006).

⁵H. Dreier, A. Dinklage, R. Fischer, M. Hirsch, P. Kornejew, and E. Pasch, *Fusion Sci. Technol.* **50**, 262 (2006).

⁶H. Dreier, A. Dinklage, R. Fischer, M. Hirsch, and P. Kornejew, *AIP Conf. Proc.* **993**, 183 (2008).